

Supplementary Information

Self-Assembly of MoO₃ Needles in Gas Current for Cubic Formation Pathway

Shinnosuke Ishizuka¹, Yuki Kimura^{1}, Satoki Yokoi², Tomoya Yamazaki¹, Rikako Sato¹ and
Tetsuya Hama¹*

1. Institute of Low Temperature Science, Hokkaido University, Hokkaido Sapporo 060-0819,
Japan

2. Department of Chemical Engineering, Graduate School of Engineering, Tohoku University, 6-
6-07 Aoba, Aramaki, Aoba-ku, Sendai, Miyagi 980-8579, Japan

Estimation of the collision frequency

Immediately after nucleation, we estimated the collision frequency between the needle-shaped particles (with long and short axes of 50 nm and 16 nm, respectively) in a simple simulation, and compared the results with the required number of attachments for cubic particle formation (~10). The attachment was induced by random Brownian motions of a needle-shaped particle in a horizontal plane.

The numerical domain is shown in Figure S9. A periodic boundary condition was imposed, and 9 particles were randomly distributed in the domain. The velocity of the particles was set to 1 m s^{-1} and 500 m s^{-1} in two separate runs. On the side collection sheet, the nanoparticles were mainly concentrated at less than 10 cm above the evaporation source, suggesting a minimum average velocity of 1 m s^{-1} . The maximum velocity (500 m s^{-1}) was assigned as the gas velocity at 500 K. The random walk distance was assumed as the particle diameter (16 nm). The time step was then set to 16 and 0.032 ns, respectively. The random walk direction was determined from a random number calculated by a standard random number generator in FORTRAN 90. When two particles approached within 26 nm, they were assumed to have collided. Note that coalescence was not considered in the particle-movement calculations.

When the particles moved at 1 m s^{-1} and 500 m s^{-1} in the horizontal plane, the number of collisions in 0.1 s was 10^5 and 10^7 , respectively. The number of collisions is linearly related to the particle velocity, suggesting that the number of collisions between the needle particles is orders of magnitude higher than the number of attachments required to grow cubic nanocrystals from the needle particles (~ 10).

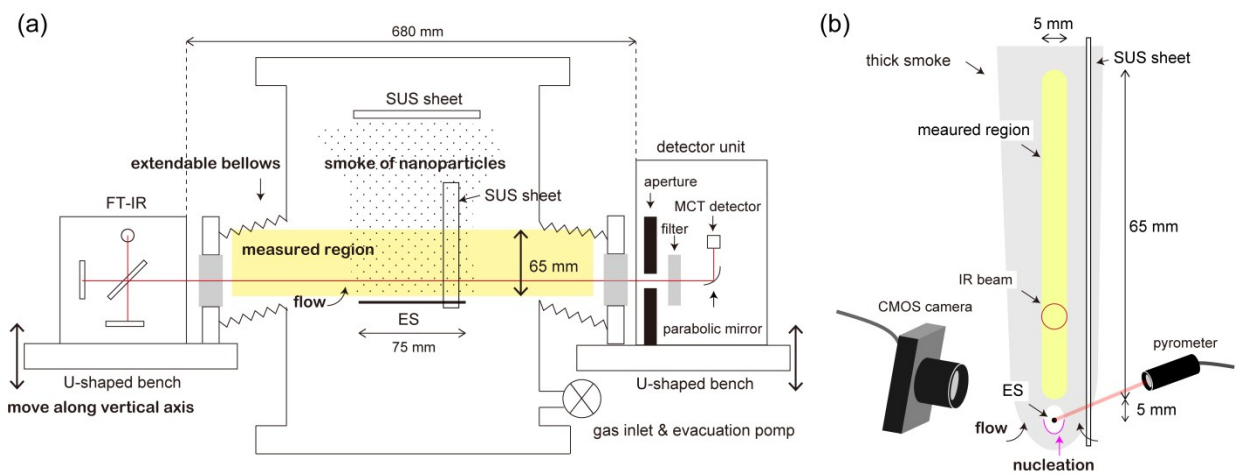


Figure S1. Schematic of (a) a side view of the experimental apparatus vertical to the optical axis and (b) smoke of nanoparticles around the evaporation source, along with the optical axis in Experiment B. The nanoparticles nucleate below or beside the evaporation source (indicated by the pink line). ES denotes evaporation source.

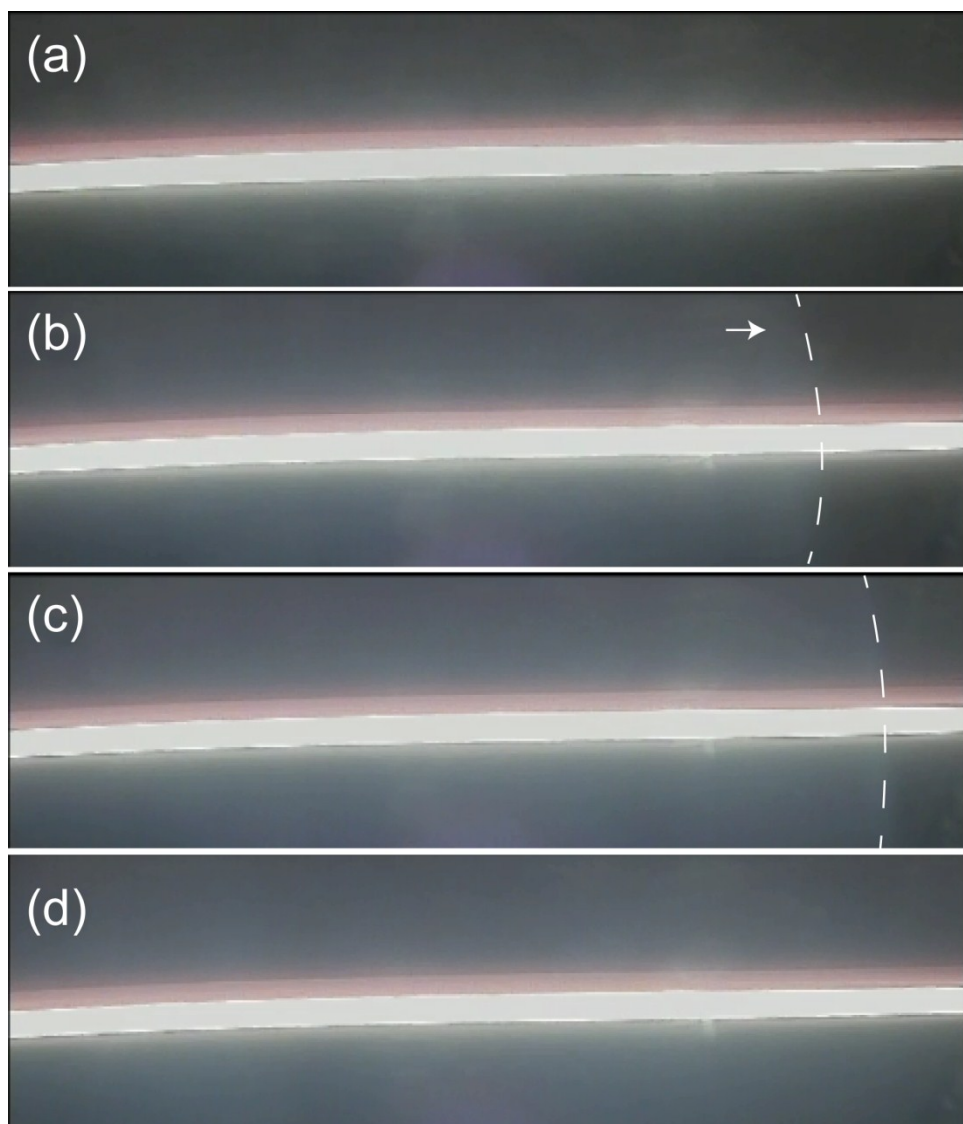


Figure S2. Snapshots of smoke nanoparticles produced in the gas current around the evaporation source shown in Figure S1(a). Horizontal bright parts belong to the evaporation source at ~ 1900 K. Taking snapshot (a) as 0 s, snapshots (b), (c), and (d) correspond to 2.0 s, 3.4 s and 5.5 s, respectively. The expanding smoke fronts are indicated by the white arrow and the dashed lines. Left of the dashed lines, the snapshots are fogged by absorption and scattering by the produced particles.

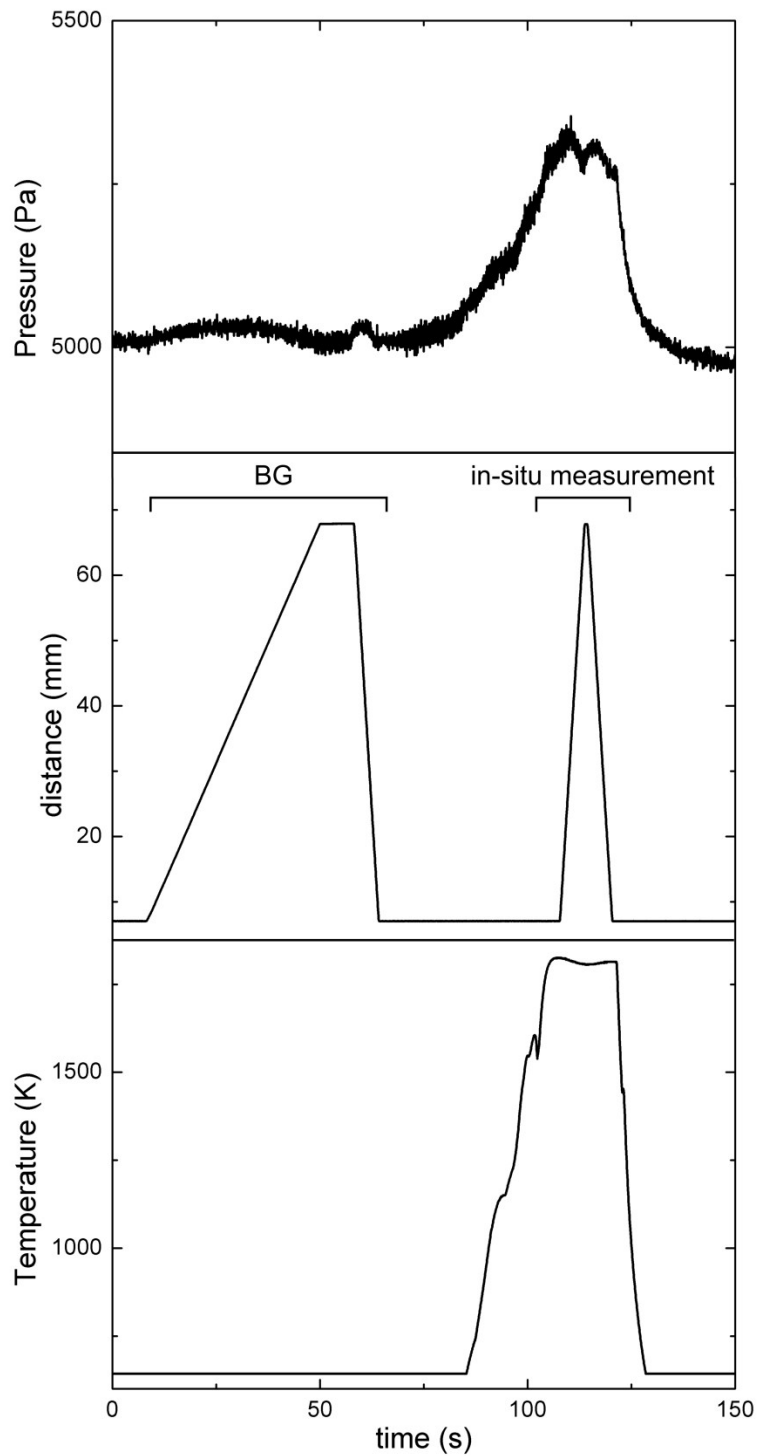


Figure S3. Time variations of the pressure in the experimental chamber, measuring position of IR spectra from the evaporation source, and temperature of the evaporation source during Experiment B.

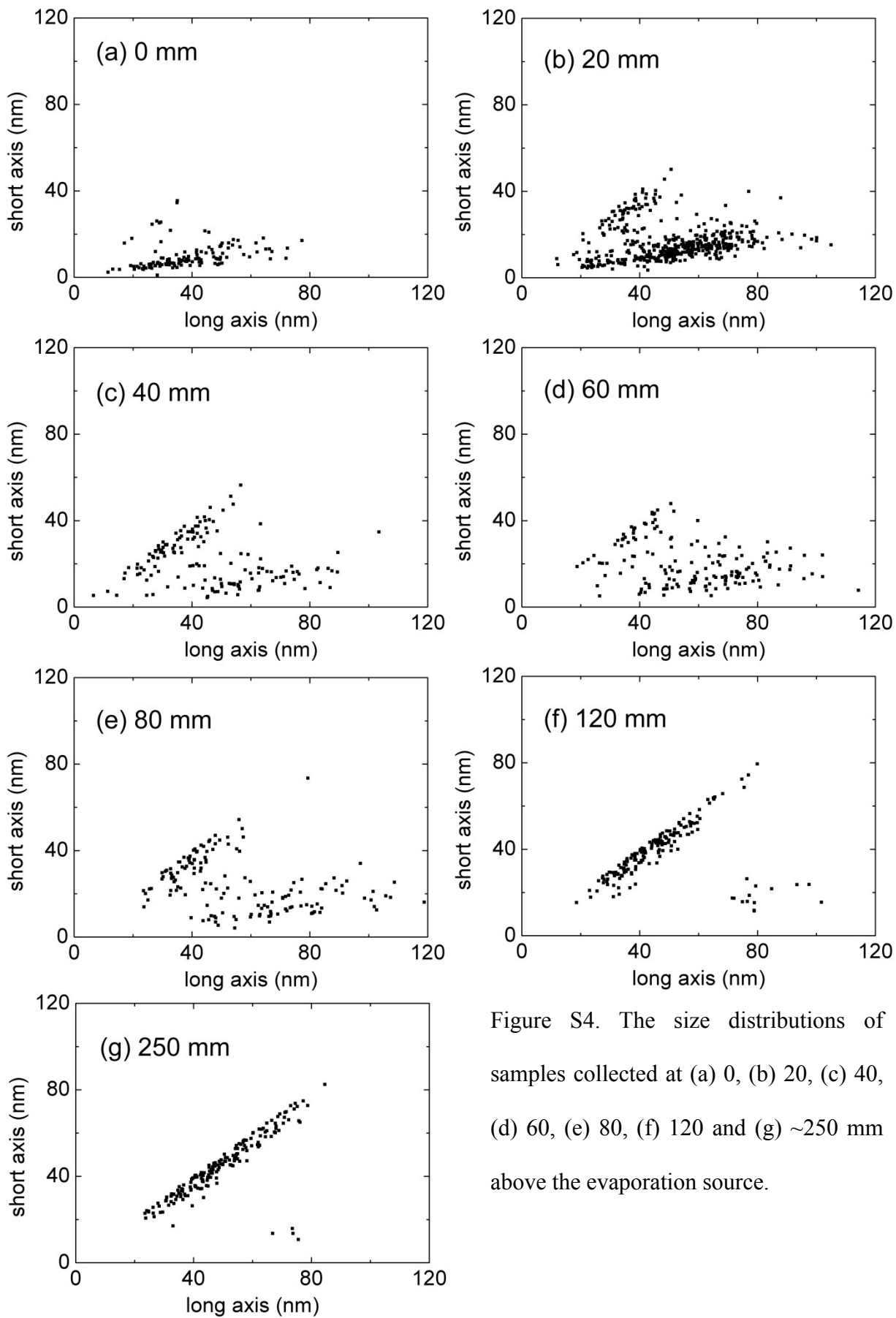


Figure S4. The size distributions of samples collected at (a) 0, (b) 20, (c) 40, (d) 60, (e) 80, (f) 120 and (g) ~250 mm above the evaporation source.

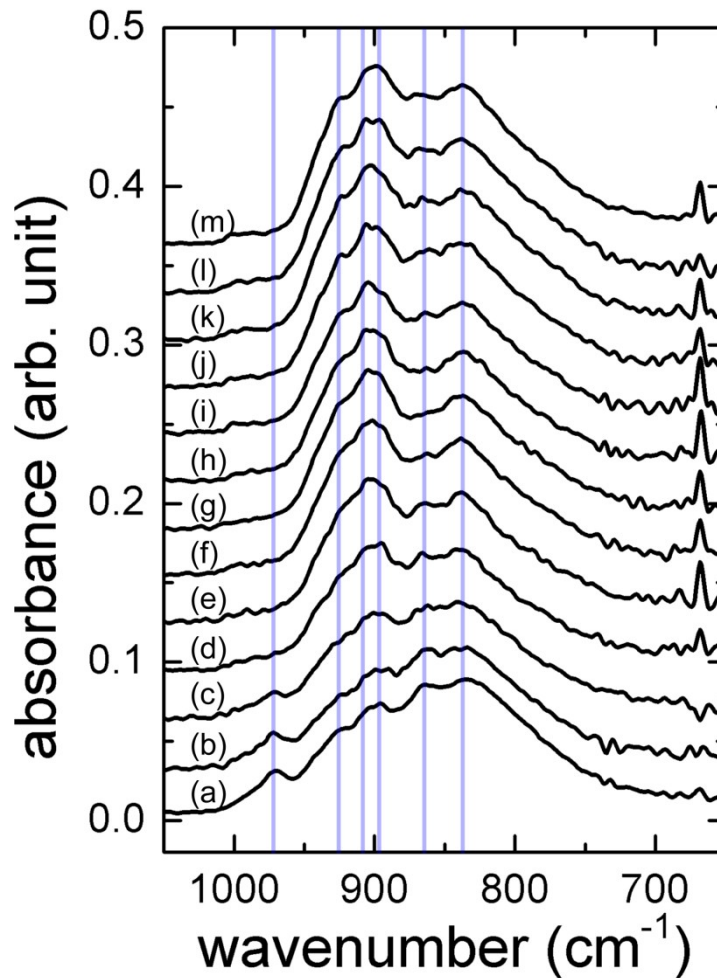


Figure S5. In-situ FT-IR spectra of nucleating and growing MoO₃ nanoparticles in the gas current obtained in the upward direction from 7.5 to 67.5 mm above the evaporation source. Measurement points are at (a) 7.5, (b) 12.5, (c) 17.5, (d) 22.5, (e) 27.5, (f) 32.5, (g) 37.5, (h) 42.5, (i) 47.5, (j) 52.5, (k) 57.5, (l) 62.5, and (m) 67.5 mm above the evaporation source in Experiment B. . Blue lines indicate the peaks at 970, 920, 910, 900, 860, and 840 cm⁻¹.

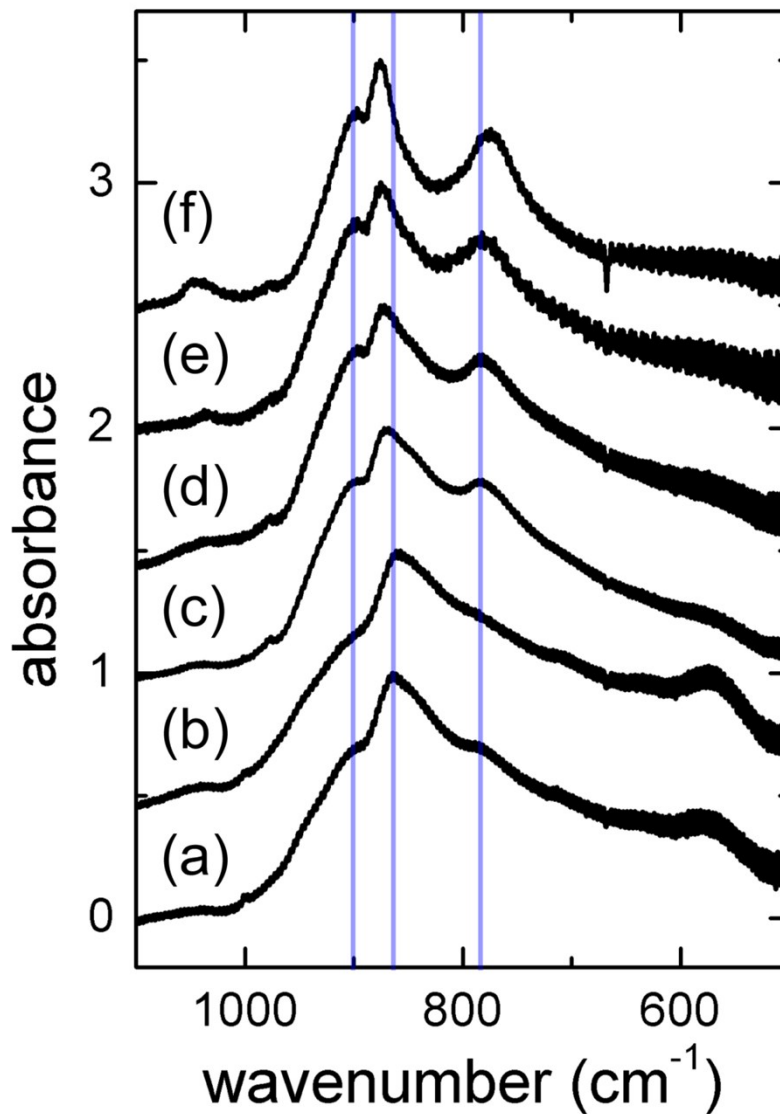


Figure S6. Normalized ex-situ IR spectra of MoO_3 nanoparticles embedded in KBr pellets. The nanoparticles were collected at (a) 20 mm beneath the evaporation source, at (b) 0 mm, (c) 30–50 mm, (d) 60–80 mm, and (e) 100–150 mm above the evaporation source on the side collector (a SUS sheet set besides the evaporation source), and at (f) more than 250 mm above the evaporation source on the roof collector (a SUS sheet set at the top of the chamber). Blue lines indicate the peaks at 900, 860, and 780 cm^{-1} . The periodic small vibrations on the spectra arise from internal reflection in the KBr pellets.

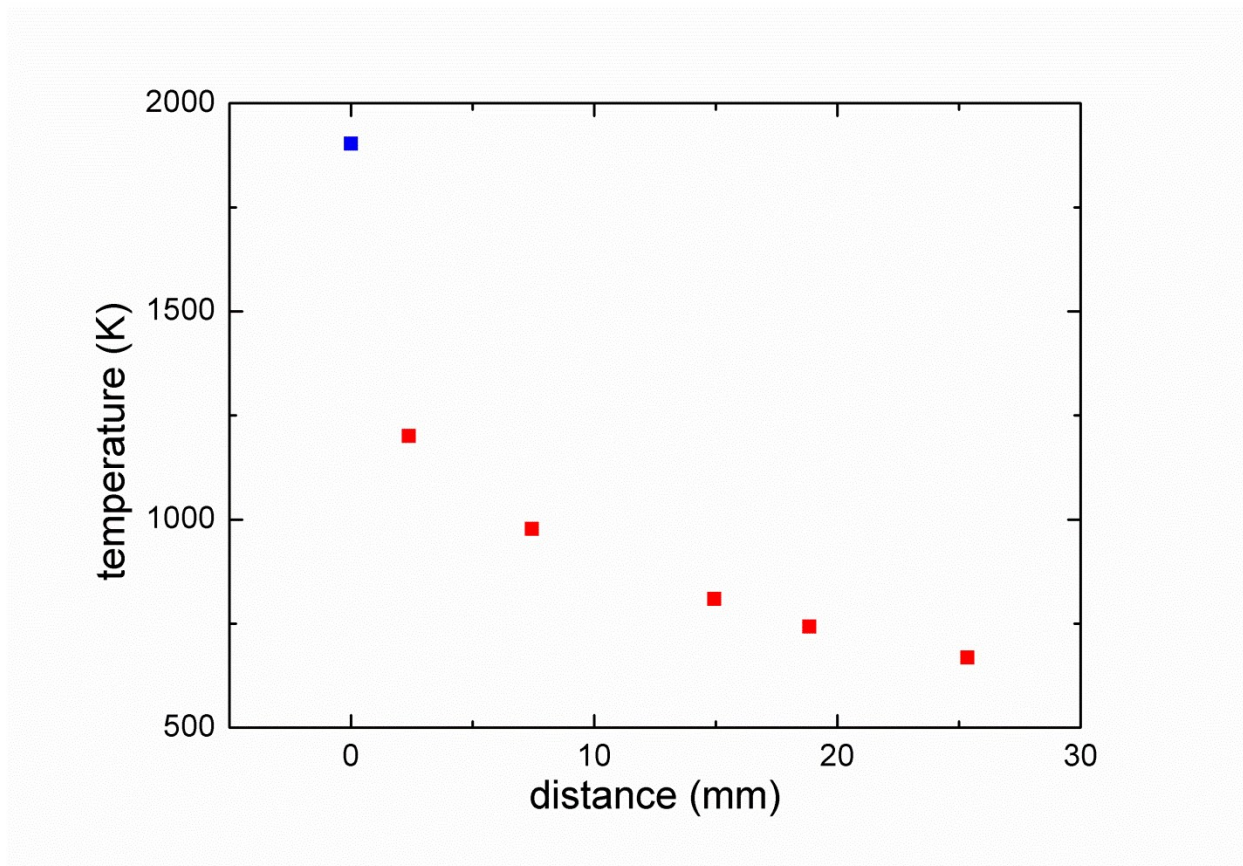


Figure S7 (red squares) Averaged temperature versus distance from the evaporation source after thermally equilibrating the K type thermocouple. The evaporation source temperature was raised to 1900 ± 100 K in a He atmosphere at 5.0×10^3 Pa (blue square). The temperature of the evaporation source was measured by a pyrometer.

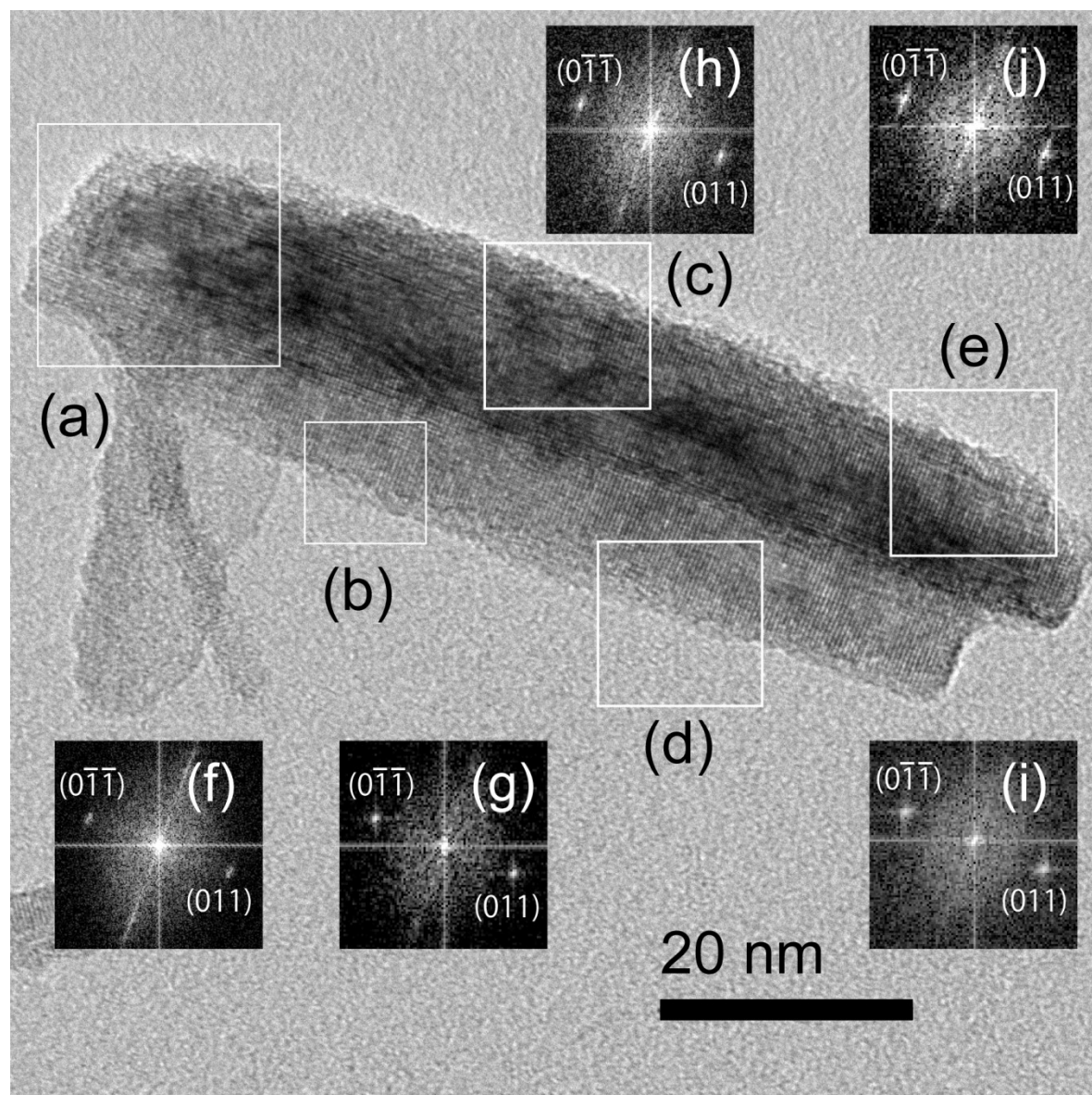


Figure S8. High-resolution image of a typical needle particle attached in the plane perpendicular to (011) . Panels (f)–(j) are FFT images of the corresponding areas enclosed in the white squares, labeled (a)–(e).

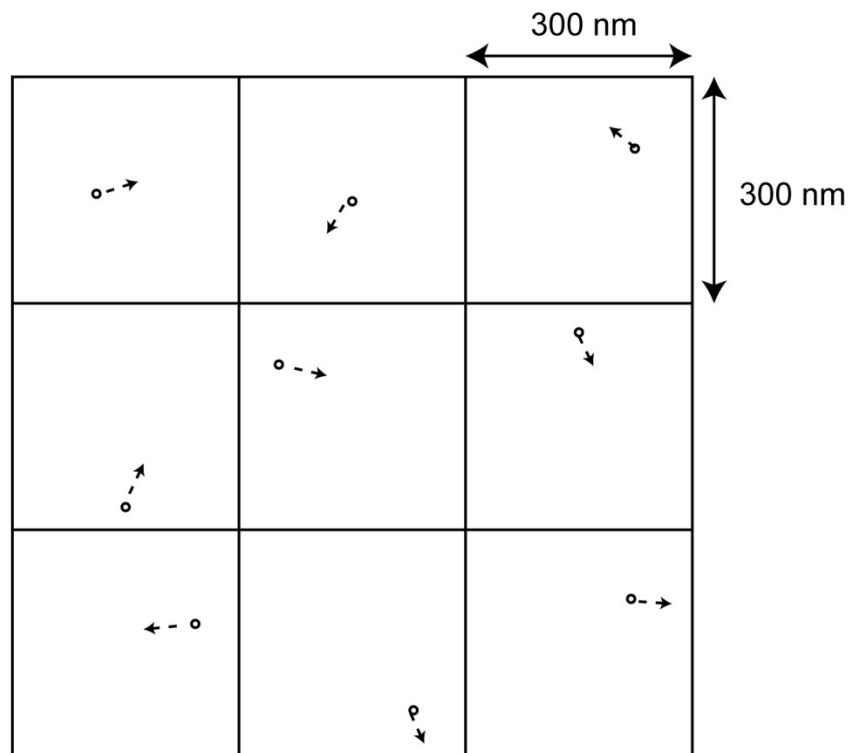


Figure S9. Initial positions of the 9 particles in the simulation.